

# Estimation of Stress Concentration Factor Using Artificial Neural Networks in T-Weld Joints Forced by Bending

Osman Bahadır ÖZDEN\*, Barış GÖKÇE

**Abstract:** Stress concentration factor (*SCF*) is a critical parameter in engineering design and structural analysis and plays an important role in determining the durability and safety of structures. In this study, a data set consisting of 8500 unique data points covering a wide range of geometric structures and parameters was created with the Latin Hypercube method in order to calculate *SCF* values with a parametric equation. The generated input data was analysed in finite element software by writing an original script recommended as a result of this study, and the resulting data was trained with an artificial neural network. The new parametric equation created at the end of the study has an average error of 4.95%. As a result, in this study, the effect of welding geometry parameters in T-welded joint *SCF* applications was examined and a parametric equation created for ease of calculation and accuracy was proposed. It is also recommended to apply *SCF* calculations with the FEA script and the original script used in this study.

**Keywords:** finite element analysis; full automation scripts; stress concentration factor; welded joints

## 1 INTRODUCTION

In welded connections, fatigue life estimation can be made using methods called nominal stress, hotspot and effective notch method, according to the recommendations of the International Welding Institute (IIW) [1]. Effective notch method is a type of geometry modelling defined by a 1 mm weld tip radius. Fatigue class is taken as 225 MPa and life is estimated. In this method, the tension at the weld tip is taken as basis. In real life, weld geometries may vary in stress concentration depending on parameters such as different angles, throat thickness, weld penetration, work and main material thickness. This can be determined by finite element analysis or by different proposed parametric equations. The stress concentration factor (*SCF*) used to compare the nominal stress and the stresses at the weld tip varies depending on the parameters. *SCF* calculations represent a critical cornerstone in the field of engineering design and structural analysis. These calculations, which examine the localized increase in stress within structural components, are of great importance due to their profound impact on the durability and safety of engineering systems. *SCF* calculations can be determined by 3 methods: experimental studies, empirical equations and finite element method [2]. Making correct decisions regarding the fatigue life of *SCF* structures, which is a very important factor in ensuring long-term reliability, is possible by understanding and correctly determining *SCF* [3]. The structural integrity of various components and systems depends primarily on the correct assessment of *SCF* [4]. High *SCF* values may indicate areas of high stress concentration, which may herald structural failure or fatigue-induced damage. Therefore, researchers largely examine accurate *SCF* and fatigue factor calculations in their quest to create strong and durable structures [5]. In addition to its importance in ensuring structural reliability, *SCF* influences fatigue life prediction [6]. Fatigue life prediction, an important aspect of welded joints, requires a comprehensive understanding of *SCF* as it directly affects the initiation and propagation of fatigue cracks [7]. Determining these values is also important in terms of time consuming and cost [8]. Studies on *SCF* calculations have been ongoing for many years. There are many methods in

the literature to determine *SCF* values in welded connections. Some studies have created new parametric equations with regression analysis [9, 10]. In some studies, training is performed with an artificial neural network (ANN), weight and bias matrices are determined and estimated with a parametric equation according to the transfer function [11, 12]. Additionally, studies have been carried out to detect *SCF* in many different geometries and strain types such as butt weld, T-weld, cruciform weld, misalignment weld [13-15]. Most of the studies are carried out with finite element analysis and the results are evaluated according to the determined parameter ranges. Here, the number of analyses becomes important for more accurate determination of *SCF* values. Additionally, mesh quality and size values are also very important when determining stress. Among the studies found in the literature, Brennan [10] proposed a parametric formula for bending stress in T-joint. The weld angle is between 30 and 60 degrees and he proposed the parametric formula in the Eq. (1) as a result of performing regression analysis with 80 data.

$$SCF = 1.01 + 0.344\alpha^{0.336} (r/t_1)^{-0.468} (L/t_2)^{0.233} \quad (1)$$

Monahan [16] performed regression analysis between weld angle 30 and 60 degrees in bending forced gold T-joint and proposed the parametric formula given in Eq. (2).

$$SCF = 1 + 0.512\alpha^{0.572} (r/t_1)^{-0.469} \quad (2)$$

Wang [9] performed regression analysis between weld angle 20 and 90 degrees in T-joint under bending stress and proposed the parametric formula given in Eq. (3) with 400 data.

$$SCF = 1 - 1.130 f(T/t) f(r_1/t) f(\theta_1) f((r_1/t)(\theta_1)) \cdot f(L_1/t) f(L_2/t) f((L_1/t)(L_2/t)) \quad (3)$$

While *SCF* calculations are made in welded connections, they are made depending on many geometric

connections. Main material thickness, workpiece thickness, weld throat thickness, weld angle, weld tip radius, weld penetration etc. parameters affect concentration values. For this reason, it becomes important to formulate it based on these parameters. Authors have been developing empirical formulas for *SCF* values for decades. Nowadays, with increasing finite element analysis capabilities, analyses can be applied through scripts. With scripts written in programming languages, different criteria can be set and more accurate and more data can be obtained. Thus, time saving and high accuracy finite element analysis results can be obtained with the data prepared through scripts. Thanks to this capability, data suitable for regression analysis can be provided. This study was carried out not only to determine *SCF* values but also to shed light on their relationship with fatigue life predictions. By rigorously analysing and comparing *SCF* calculations under varying geometries and key parameters, this research aims to provide valuable information that will enable researchers to make more accurate decisions in design processes, ultimately increasing the safety, reliability and longevity of engineering structures. *SCF* determinations are possible with the new parametric equation determined by an artificial neural network. In addition, the methodology implemented with the script algorithm created for the parametric equation was recommended for *SCF* determinations as a result of this study.

## 2 NUMERIC ANALYSIS AND PREPARED DATA'S

Ansys 2022 R2 software, a finite element software, was used for numerical analysis. Parameters that will affect weld tip stresses and *SCF* values have been determined. The ranges of the specified parameters were determined and equal data distribution was ensured with the method called the Latin Hypercube method. This method is used in many studies in the literature [17]. These data, distributed evenly at specified intervals, were saved in a file as input. Matlab software was used for data preparation with the Latin Hypercube Method. With this method, 8384 data distributions were created according to the intervals determined. The parameters and parameter ranges determined for this data are shown in Fig. 1.

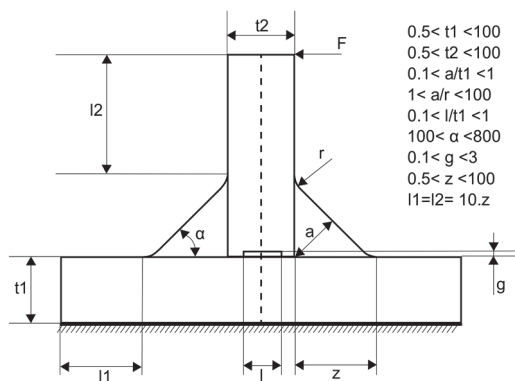


Figure 1 Welded joints FEA Modelling

According to the parameters and ranges shown in Fig. 1, the data were distributed equally with the Latin Hypercube method. The precision of these data is defined

as 5 degrees in the angle parameter and 0.1 mm in other parameters. From the distributed data,  $a/r$  and  $a/t_1$  with 0.1 mm precision are shown in Fig. 2. Finite element analysis was applied to all data via script according to the determined indexes.

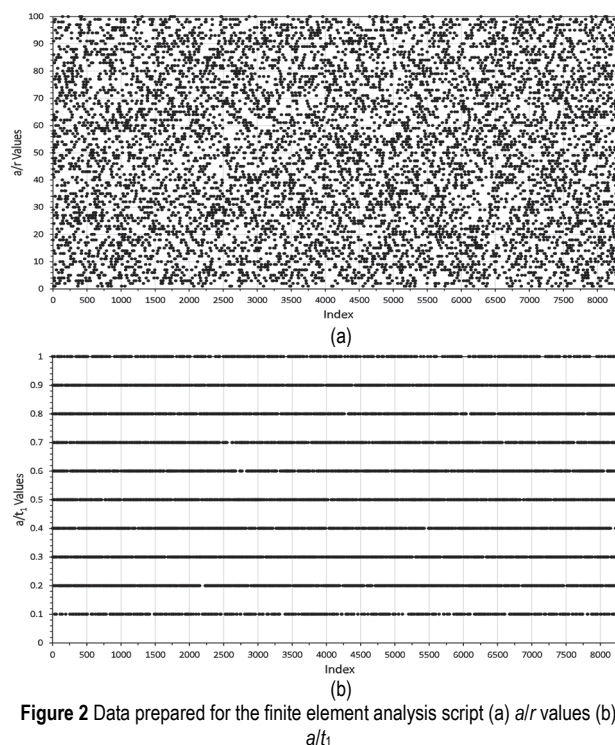


Figure 2 Data prepared for the finite element analysis script (a)  $a/r$  values (b)  $a/t_1$

While determining *SCF* values, the region at the weld end, which is the nominal stress and maximum stress region, was taken as basis. *SCF* values were determined using Eq. (4). The nominal stress value was found by drawing a linear line to points 80 mm and 100 mm away from the welding tip. These points are the points that are minimally affected by the parameters.

$$SCF = \frac{\sigma_{\max}}{\sigma_{\text{nominal}}} \quad (4)$$

A script that communicates CAD and CAE software for numerical analysis has been prepared. This script was prepared with the Python programming language and commands were given with the Command Window in Ansys Workbench software. In this command, the scripts prepared separately for CAD and CAE are processed sequentially. With this communication, it is possible to update the geometry according to the input data prepared and to perform analysis in CAE. Input data was obtained by communicating with a .txt extension file. In this way, a large number of data can be analysed sequentially. These parameters prepared in Fig. 1 were defined as input with a script in Spaceclaim, a CAD software. After the geometry is defined, CAE is updated and automatically reduces the mesh size value if it does not meet the criteria before the mesh is created. The mesh criterion is determined as 0.93 according to the criterion called element quality, and the mesh size value is reduced by 0.1 mm until this criterion is met. Mesh convergence was performed before making analysis based on input data. The value where the number

of meshes is high and the tension becomes stable is defined as the default mesh. If it does not meet the criteria after the iterations start, this default value is changed by decreasing the mesh size. After the mesh criterion was defined, weld end stresses and SCF values were recorded as output data

according to the nominal stress, hotspot stress and effective notch stress methods. The flow chart of this fully automated and recommended method is shown in Fig. 3. Iterations are defined as  $i$  and the last iteration, the  $i$  value determined according to the generated data, is 8384.

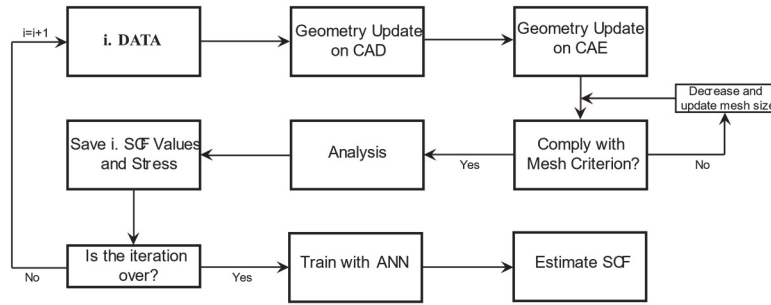


Figure 3 Proposed full automation SCF acquisition flow chart

With the completion of the iterations, numerical analysis was completed and the input data obtained was 7. As the output value, it is the nominal stress value determined according to the weld tip tension and the points 80 and 100 mm away. According to these stresses, SCF values were determined for all data. The data obtained was created for training with ANN. ANN is defined according to the Levenberg-Marquart algorithm. 7 inputs ( $a, r, l, t_1, t_2, g, \alpha$ ), 2 hidden layers and 1 output (SCF) are defined. There are 5 neurons in each hidden layer. The activation function is defined according to the linear purelin function. The training was carried out with the Matlab neural network toolbox and was implemented as feedforward and backpropagation. As a result of many trials, it was determined that the error rate was low and these values were taken according to the trials. All definitions were performed after the training was completed to obtain bias ( $b_i$ ) and weight matrices ( $W_i$ ). Input values are normalized between 1 and -1 and are denormalized when estimating the output. In addition,  $X_{gain}, X_{offset}, Y_{gain}$  and  $Y_{offset}$  matrices were determined for normalization and denormalization processes. Thus, a new SCF parametric formula is aimed with ANN training. After all training is completed and the specified matrices are obtained, the formula used for SCF estimation is given in Eq. (5) to Eq. (8). The ANN structure specified by equations and used for SCF training is shown in Fig. 4.

$$a_2 = b_2 + w_2 \tan sig(a_1) \tag{6}$$

$$a_3 = b_3 + w_3 \tan sig(a_2) \tag{7}$$

$$SCF = \text{purelin}(a_3) Y_{gain} + Y_{offset} \tag{8}$$

Comparisons were made for all data according to the parametric formula determined as a result of ANN training. The average error rate obtained for these comparisons is given in Eq. (9). In addition, for comparison of statistical data, root mean square error (RMSE) in Eq. (10), correlation square given in Eq. (11).

$$\text{error}_{rate} = \frac{SCF_{estimation} - SCF_{FEA}}{SCF_{FEA}} \tag{9}$$

$$RMSE = \sqrt{\frac{1}{p} \sum_j |t_j - o_j|^2} \tag{10}$$

$$R^2 = 1 - \left( \frac{\sum_j (t_j - o_j)^2}{\sum_j (o_j)^2} \right) \tag{11}$$

$$a_1 = b_1 + w_1 (\text{input} \cdot X_{gain} + X_{offset}) \tag{5}$$

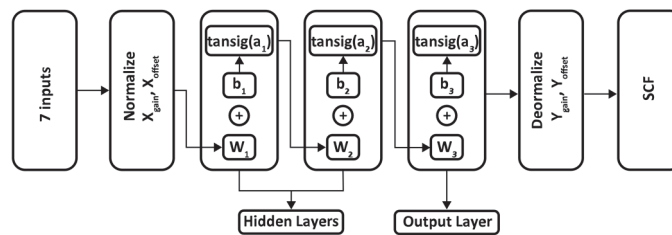


Figure 4 Schematic structure of the artificial neural network used for SCF training

### 3 RESULTS AND DISCUSSION

With the determined parameter ranges, 8500 pieces of data were distributed equally with the Latin Hypercube

method. By running the full automation script, 1.72%, i.e., 116, were the perpetrators. The reason for these errors is due to geometric irregularity and 8384 numerical analysis

results were obtained. This geometric irregularity means that such a geometry cannot be achieved in real life.

Additionally, nominal, effective notch and hotspot tension values were recorded. Thus, *SCF* values were obtained based on the weld tip stress. The data obtained through numerical analysis was trained with ANN. ANN was trained with a number of epochs of 1200000. As a result of the training, bias and weight matrices were determined to obtain a new parametric formula. The detected bias and weight matrices are given in Eq. (12) to Eq. (21).

$$X_{\text{offset}} = \begin{bmatrix} -1.01309 \\ -1.00205 \\ -1.01112 \\ -1.08333 \\ -1.01566 \\ -1.06897 \\ -1.28480 \end{bmatrix} \quad (12)$$

$$X_{\text{gain}} = \begin{bmatrix} 0.02013 \\ 0.02053 \\ 0.02021 \\ 0.02083 \\ 0.02016 \\ 0.68966 \\ 0.02910 \end{bmatrix} \quad (13)$$

$$Y_{\text{offset}} = [8.88498] \quad (14)$$

$$Y_{\text{gain}} = [8.41733] \quad (15)$$

$$b_1 = \begin{bmatrix} 1.95870 \\ -7.22786 \\ -5.78728 \\ -1.61206 \\ -2.51554 \end{bmatrix} \quad (16)$$

$$b_2 = \begin{bmatrix} -4.82921 \\ -5.42331 \\ -92.51923 \\ -4.97471 \\ -11.90807 \end{bmatrix} \quad (17)$$

$$b_3 = [-1.69977] \quad (18)$$

$$W_1 = \begin{bmatrix} 0.00386 & 0.72168 & 0.01963 & 0.01267 & 0.76857 & -0.00598 & -0.12925 \\ -1.61657 & -4.61120 & -1.53535 & -0.06825 & 1.27604 & 0.05470 & -0.15247 \\ -0.04695 & -4.46091 & -0.0404 & 0.00736 & 0.21790 & -0.00018 & -0.03177 \\ -0.11896 & 0.10904 & -0.02632 & -0.03339 & -0.49323 & 0.00537 & 0.38689 \\ -0.34998 & -0.58323 & -0.03092 & -0.02323 & -0.53235 & 0.01533 & 0.14065 \end{bmatrix} \quad (19)$$

$$W_2 = \begin{bmatrix} -0.51306 & 0.17963 & -7.77940 & -1.13517 & 0.73916 \\ 0.12723 & 0.18191 & -7.50701 & 0.49374 & -0.14122 \\ -53.84110 & 6.34260 & -10.18365 & 47.77993 & -195.90499 \\ -0.07537 & 0.17265 & -7.30731 & 0.00660 & 0.11947 \\ 4.97945 & -4.51778 & 1.30333 & 22.72586 & -38.48509 \end{bmatrix} \quad (20)$$

$$W_2 = [59.16282 \quad 20.80761 \quad -38.74768 \quad -54.42614 \quad 13.86126] \quad (21)$$

Eq. (12) to Eq. (21), the matrices obtained as a result of ANN training and *SCF* values at the weld end are obtained with the equations given in Eq. (5) to Eq. (8). Thus, the *SCF* parametric formula was obtained. With the parametric formula error rates were determined with Eq. (9). Additionally, statistical comparisons were compared

with the equations given in Eq. (9) to Eq. (11). Fig. 5a shows the distribution of the differences between target and output values. Fig. 5b shows the comparison of the *SCF* value (output) of the new parametric equation and the FEA result (target) as a result of ANN training.

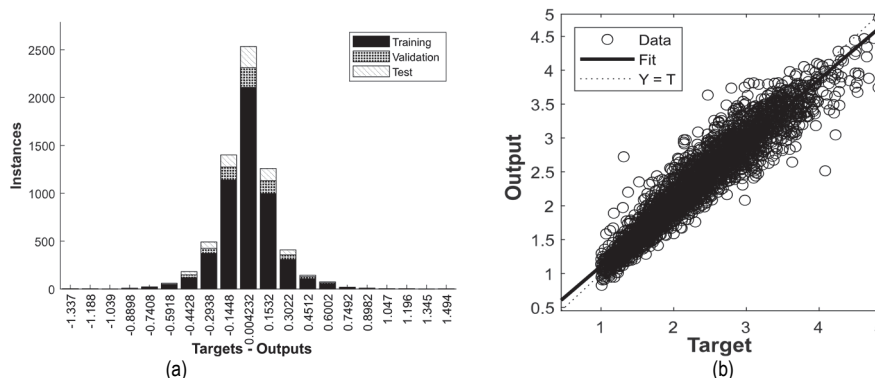


Figure 5 Parametric equation results (a) target-outputs difference distribution (b) data on target-output

The maximum *SCF* value was determined as 4.95. The minimum *SCF* value was determined to be 1.001. All data

were compared according to the output results obtained as a result of this training. Statistical data were determined by

Eq. (9) to Eq. (11). According to the newly created parametric *SCF* as a result of ANN training, the average error value was determined according to the equation given in Eq. (9) and was found to be 4.95%. *RMSE* value was determined as 24.57% and correlation square value was 95.72%. Each of 7 different parameters is effective in *SCF* values. Especially the radius value at the weld tip may change after welding. It may vary depending on the weld throat thickness. *SCF* values are given based on *a/r* parameters according to the proposed parametric equation trained with ANN shown in Fig. 6. It was prepared according to the equation  $l = 1, g = 2, \alpha = 45, t_1 = t_2,$  and  $t_1 = 1.4 a.$  The weld neck (*a*) was examined at 5, 7, 10, 20, 30 and 50 mm. *a/r* was examined with a sensitivity of 1 between 1 and 100. According to these results, it was determined that it exhibited a non-linear behaviour according to the *a/r* parameter. It has been determined that *SCF* increases as the weld throat thickness increases, and *SCF* decreases as the radius at the weld tip increases. It is seen that these examined parameters are very effective, especially in cases of different radii and throat thicknesses that may occur after welding.

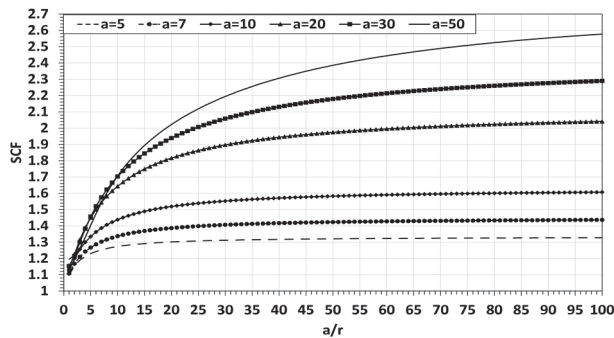


Figure 6 Stress concentration factor values according to *a/r* parameter

The proposed equation to determine the effect of the welding angle and its variation with thickness is shown in Fig. 7. It was prepared according to the equation  $l = 1, g = 2, t_1 = t_2, r = 1$  and  $t_1 = 1.4a.$  It has been determined that as the welding angle increases, *SCF* values change according to the weld throat thickness. It is seen that the effect of the welding angle increases as the throat thickness increases. While the *SCF* change rate was 7.39% at  $a = 5$  mm, it was found to be 47.50% at  $a = 50$  mm.

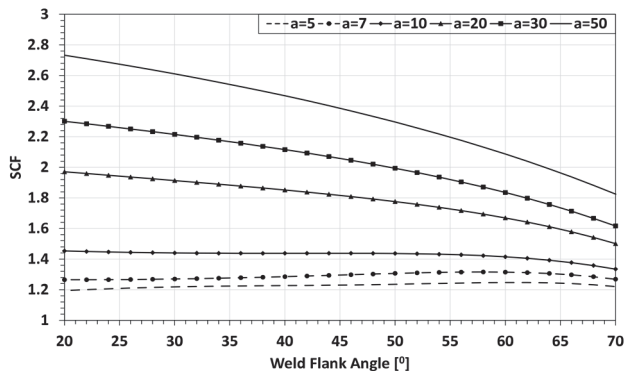


Figure 7 Stress concentration factor values according to weld angle

Weld penetration effects are shown in Fig. 8. It was prepared according to the equation  $g = 2, \alpha = 45, t_1 = t_2, r = 1$  and  $t_1 = 1.4a.$  It has been determined that the *SCF*

value decreases as weld penetration increases, but its effect varies depending on the weld throat thickness. According to the data taken between 0 - 1  $l/t_1$  ratio, it was determined that the *SCF* change was 14.09% at 5 mm throat thickness and 2.35% at 50 mm throat thickness. It is seen that as the weld thickness increases, the weld penetration effect decreases.

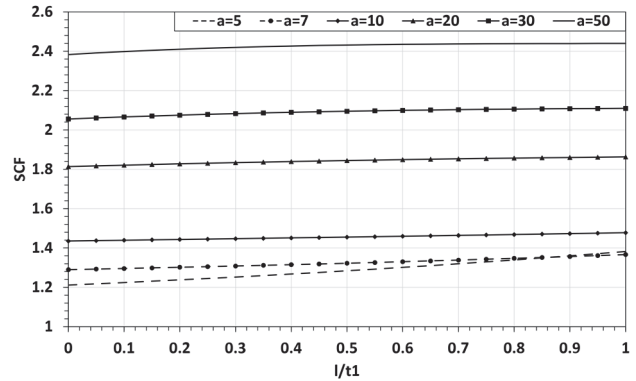


Figure 8 Stress concentration factor values according to weld penetration effects

The  $r/t_1$  ratio for the effects of radius values at the weld end is shown in Fig. 9, according to changes between 0.05 and 0.8. Fig. 9a shows the weld throat thickness and (b) shows its effects according to  $t_2/t_1$ . Fig. 9a,  $l = 1, g = 2, \alpha = 45, t_1 = t_2,$  and  $t_1 = 1.4a$  and (b),  $l = 1, g = 2, \alpha = 45, t_1 = 10$  and  $t_1 = 1.4a$  were prepared according to equations.

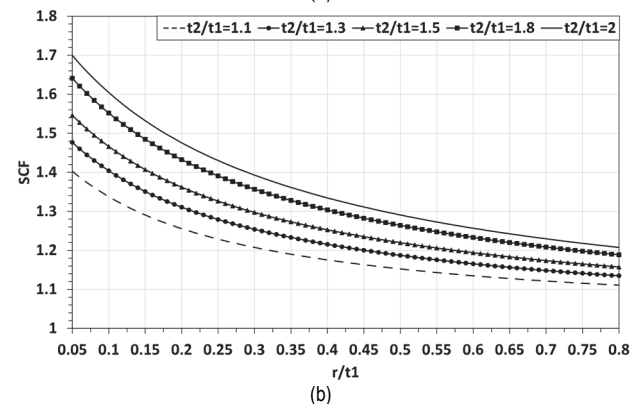
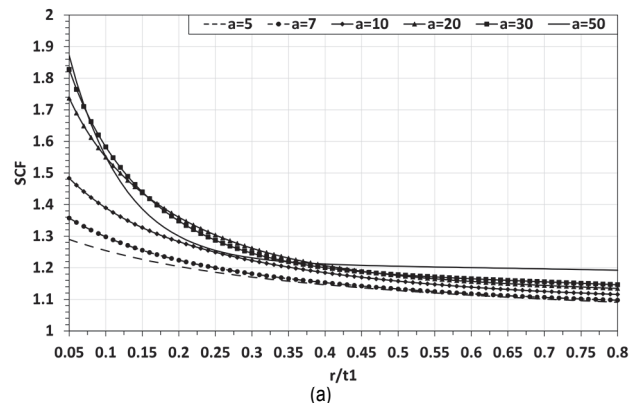


Figure 9 *SCF* values according to weld penetration

It is seen that the *SCF* value increases as the thickness increase rate between the workpiece and the main material increases. The *SCF* value is less when the values are close to each other. In addition, it is seen that increasing the weld tip radius value according to these thickness ratios also

decreases the *SCF* value. There is a nonlinear behaviour in weld throat thickness changes. While a low throat thickness creates less impact on *SCF*, its effects increase as the thickness increases. ANN estimates and probability results for *SCF* normal distribution were compared with other studies in the literature as shown in Fig. 10 [9, 10, 16]. The standard deviation was determined as 0.09 in ANN. According to the parametric formula suggested by Wang, a standard deviation value of 0.841 was determined and the closest results are in this study. Standard deviation values were determined as 2.095 in the Monahan formula and 1.431 in the Brennan formula.

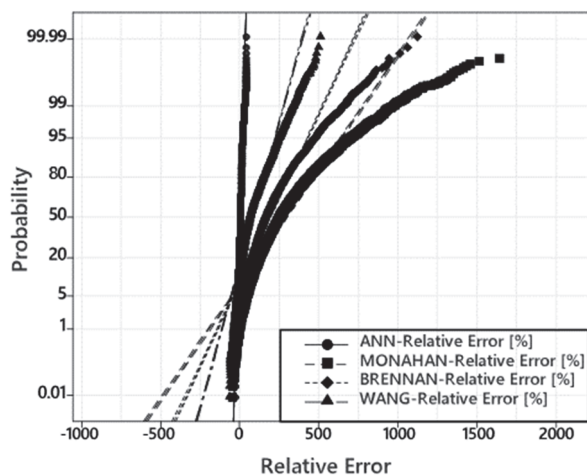


Figure 10 Probability plot of the relative errors for normal distribution

Comparisons with ANN, Monahan, Brennan and Wang parametric formulas are shown as a boxplot in Fig. 11. Median values were determined as 0.002 in ANN, 2.491 in Monahan, 1.623 in Brennan and 0.627 in Wang. Additionally, lower quartile (Q1) and upper quartile (Q3) values were determined as shown in the boxplot in Fig. 11. Q1 values were determined as -0.046 in ANN, 1.487 in Monahan, 0.906 in Brennan and 0.200 in Wang. Q3 values were determined as 0.052 in ANN, 3.930 in Monahan, 2.631 in Brennan and 1.291 in Wang.

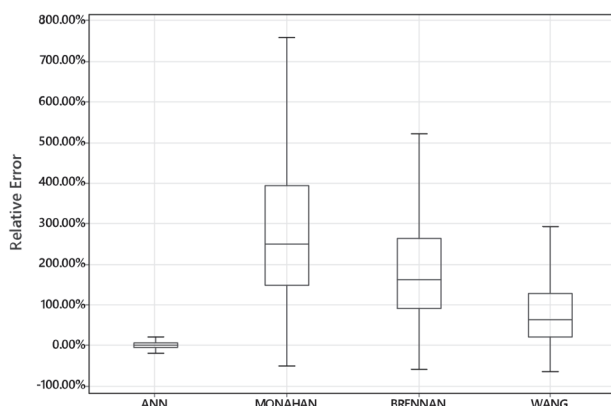


Figure 11 Comparisons for boxplot values

There are high differences in the parametric formulas of Brennan and Monahan from other studies. This may be due to the difference in boundary conditions or the small number of data. In addition, in this study, parameters were defined with much wider ranges and mesh criteria were added to the script. For this reason, there are differences in

comparing the results. Input data were defined at wider intervals compared to other studies before being distributed equally with the Latin hypercube method. 8384 data were created and more data was provided than many studies in the literature [10, 16, 17]. Therefore, the new parametric equation created provides more accurate results. The boundary conditions and bending force in which the study was carried out are the originality of this study. Due to different boundary conditions, stress concentration factor values are different compared to other studies [13, 15, 18]. In the comparisons in Fig. 10 and Fig. 11, it was observed that the error rates differ due to boundary conditions. The new equation created is valid for these conditions. In addition, while in some studies the data were distributed with full penetration definitions, in this study the data were defined based on the penetration rate. Thus, in the newly created parametric equation, a more comprehensive equation was obtained according to new boundary conditions. The scenarios were prepared according to the algorithm specified in the flow chart in Fig. 3, which is new and different from other studies in the literature [17, 18]. CAE analyses the parameters determined by the Latin Hypercube method with a script, while checking the mesh criteria in each analysis. As the number of mesh nodes and elements increases, stress increases up to a certain value. In this script, peak stress values were detected more accurately thanks to the mesh criterion. These quality values have been neglected in other studies in the literature. The reason for this is that they apply the CAE software without checking it with the script. In this study, the criterion was controlled by script. In this way, more accurate and abundant data was obtained.

#### 4 CONCLUSION

In this study, input data for *SCF* detection was set in the ranges determined by 7 parameters with the prepared T-welded joint geometry. According to this input data, finite element analyses were applied with a script that controls CAD and CAE software. In each analysis, an algorithm that will not reduce the mesh quality criterion is defined. In each analysis, an algorithm that will not reduce the mesh quality is defined. In each analysis, the script recorded the nominal stress and the stresses in the weld notch. It was trained with ANN, whose outputs were prepared as a result of the analysis made with 8384 data obtained. As a result of the training, bias and weight matrices were obtained. These matrices were compared by substituting them with the specified formula according to the defined activation function. As a result of the comparisons, the average error value was determined as 4.95% and the *RMSE* value was 24.57%. As a result of this study, a new parametric equation with 7 input parameters was obtained for the T-welded joint notch *SCF*. The results of the effect of 7 parameters on the *SCF* value are presented according to this parametric equation trained on the artificial neural network. These findings were compared with some studies in the literature and their statistical parameters. In addition, the unique script algorithm applied in this study is recommended because it is quite efficient for *SCF* values and provides more accurate results. Unlike other studies in the literature, mesh quality criteria for *SCF* values were checked with a script for the first time, and this

methodology was proposed to provide more data and more accurate results in *SCF* determinations. In future studies, parametric equations can be created for different weld types, boundary conditions and loading types according to this proposed code algorithm.

## Acknowledgements

The authors gratefully acknowledge the support of "MPG Machinery Production Group Inc. Co. " in this study. This work has been supported by Necmettin Erbakan University Scientific Research Projects Coordination Unit under project number 23DR19005.

## 5 REFERENCES

- [1] Hobbacher, A. (2016). *Recommendations for fatigue design of welded joints and components*, 47. Springer. <https://doi.org/10.1007/978-3-319-23757-2>
- [2] Kolios, A., Wang, L., Mehmanparast, A., & Brennan, F. (2019). Determination of stress concentration factors in offshore wind welded structures through a hybrid experimental and numerical approach. *Ocean Engineering*, 178, 38-47. <https://doi.org/10.1016/j.oceaneng.2019.02.073>
- [3] Hectors, K. & De Waele, W. (2020). A numerical framework for determination of stress concentration factor distributions in tubular joints. *International Journal of Mechanical Sciences*, 174, 105511. <https://doi.org/10.1016/j.ijmecsci.2020.105511>
- [4] Wang, Y., Luo, Y., Kotani, Y., & Tsutsumi, S. (2021). Generalized *SCF* formula of out-of-plane gusset welded joints and assessment of fatigue life extension by additional weld. *Materials*, 14(5), 1249. <https://doi.org/10.3390/ma14051249>
- [5] Fricke, W. (2003). Fatigue analysis of welded joints: state of development. *Marine structures*, 16(3), 185-200. [https://doi.org/10.1016/S0951-8339\(02\)00075-8](https://doi.org/10.1016/S0951-8339(02)00075-8)
- [6] N'diaye, A., Hariri, S., Pluvinage, G., & Azari, Z. (2007). Stress concentration factor analysis for notched welded tubular T-joints. *International Journal of Fatigue*, 29(8), 1554-1570. <https://doi.org/10.1016/j.ijfatigue.2006.10.030>
- [7] Schaumann, P. & Schürmann, K. (2019). New proposal to express notch stress approach results by equivalent *SCFs*. *International Journal of Fatigue*, 119, 11-19. <https://doi.org/10.1016/j.ijfatigue.2018.09.009>
- [8] Kiraz, A., Erkan, E. F., Canpolat, O., & Kökümer, O. (2023). Prediction of stress concentration factor in butt welding joints using artificial neural networks. *International journal of research in industrial engineering*, 12(1), 43-52.
- [9] Wang, Y., Luo, Y., & Tsutsumi, S. (2020). Parametric formula for stress concentration factor of fillet weld joints with spline bead profile. *Materials*, 13(20), 4639. <https://doi.org/10.3390/ma13204639>
- [10] Brennan, F., Peleties, P., & Hellier, A. (2000). Predicting weld toe stress concentration factors for T and skewed T-joint plate connections. *International Journal of Fatigue*, 22(7), 573-584. [https://doi.org/10.1016/S0142-1123\(00\)00031-1](https://doi.org/10.1016/S0142-1123(00)00031-1)
- [11] Dabiri, M., Ghafouri, M., & Björk, T. (2017). Estimation of stress concentration factors in butt and T-welded joints using artificial neural network-based models. *Rakenteiden Mekaniikka*, 50(3), 362-367. <https://doi.org/10.23998/rm.64415>
- [12] Oswald, M., Mayr, C., & Rother, K. (2019). Determination of notch factors for welded cruciform joints based on numerical analysis and metamodeling. *Welding in the World*, 63, 1339-1354. <https://doi.org/10.1007/s40194-019-00751-y>
- [13] Molski, K. L., Tarasiuk, P., & Glinka, G. (2020). Stress concentration at cruciform welded joints under axial and bending loading modes. *Welding in the World*, 64, 1867-1876. <https://doi.org/10.1007/s40194-020-00966-4>
- [14] Pachoud, A. J., Manso, P., & Schleiss, A. (2017). New parametric equations to estimate notch stress concentration factors at butt welded joints modeling the weld profile with splines. *Engineering Failure Analysis*, 72, 11-24. <https://doi.org/10.1016/j.engfailanal.2016.11.006>
- [15] Oswald, M., Neuhäusler, J., Frey, M., & Rother, K. (2022). Determination of notch factors for welded T-joints based on numerical analysis and metamodeling. *Welding in the World*, 66(12), 2609-2624. <https://doi.org/10.1007/s40194-022-01368-4>
- [16] Neuhäusler, J. & Rother, K. (2022). Determination of notch factors for transverse non-load carrying stiffeners based on numerical analysis and metamodeling. *Welding in the World*, 66(4), 753-766. <https://doi.org/10.1007/s40194-021-01240-x>
- [17] Monahan, C. C. (1995). *Early fatigue crack growth at welds*. Computational mechanics.
- [18] Molski, K. L. & Tarasiuk, P. (2021). Stress concentration factors for welded plate T-joints subjected to tensile, bending and shearing Loads. *Materials*, 14(3), 546. <https://doi.org/10.3390/ma14030546>

### Contact information:

**Osman Bahadır ÖZDEN**, PhD Student  
(Corresponding author)  
Department of Mechanical Engineering, Necmettin Erbakan University,  
Meram, 42090 Konya/Turkey  
E-mail: bozden@mpg.com.tr

**Barış GÖKÇE**, PhD, Associate Professor  
Department of Mechatronics Engineering, Necmettin Erbakan University,  
Meram, 42090 Konya/Turkey  
E-mail: bgokce@erbakan.edu.tr